Spectroscopic and Impedance Studies of Reverse Biased Degraded Dye Solar Cells

L.J. le Roux*, D. Knoesen and S. Hietkamp

* CSIR Materials Science and Manufacturing, Energy and Processes, PO Box 395, Pretoria, 0001. Email: lleroux@csir.co.za

ABSTRACT

The work that is presented here is focused on the results that were obtained during studies of the performance of Dye Solar Cells under certain reverse bias conditions. This reverse voltage could permanently modify or damage a cell if it is not properly protected. Various techniques were employed to determine the physical changes in the cell.

It was found that a cell that was subjected to a reverse bias of 2 V for 500 minutes showed a 58% recovery. The UV-Vis spectra showed a blue shift (higher energy), the Raman showed no peak at 1713 cm^{-1} and the FT-IR showed the disappearance of the S-C-N absorption band at 2100 cm^{-1}. The combined conclusion is that the –NCS ligand has been depleted and replaced with I_3^- ions. Nyquist and Bode plots showed an increase in the charge transfer resistance at the counter electrode. This indicates a partial oxidation of the Pt catalyst on the counter electrode.

The changes in the cell after being subjected to a reverse bias potential of 2 V for 500 minutes are changes on the -NCS bonds on the Ru containing dye as well as the Pt on the counter electrode.

Keywords: Electrochemical impedance spectroscopy, Nyquist plots, Bode plots, IV-curves, Raman, FT-IR, UV-Vis, reverse bias.

1 INTRODUCTION

A dye solar cell is an electrochemical cell that generates electricity when light excites the electrons in a ruthenium containing dye (from hereon called the Ru dye) that is chemically adsorbed on a thin layer of nano-TiO_2. It consists of a working electrode (TiO_2 and dye), an electrolyte (0.1 M I_2, 0.1 M LiI, 0.6 M tetrabutylammonium iodide, 0.5 M 4-*tert*-butylpyridine in acetonitrile) and a counter electrode (platinum catalyst).

1.1 Reverse bias

Reverse bias conditions occur when the voltage across a cell opposes the open circuit potential. A multi cell module might have one or more of its cells shaded out while operating in the open. When one cell in the series connection is shaded, the current will pass this cell in reverse bias. An example of such a case can be seen in Figure 1. In such a case the shaded cell will be subjected to a voltage in the reverse direction coming from the other lit cells in the module. The reverse voltage could adversely modify or damage the cell if it is not properly protected.

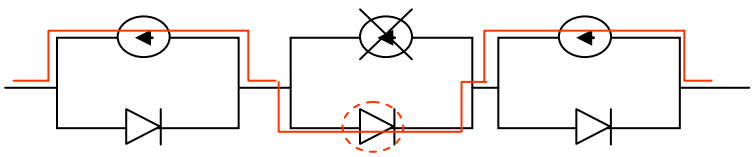

Figure 1: Example of the circuit where one cell is shaded

When a negative voltage is applied, the potential across the semiconductor increases as well as the depletion layer width. When a positive voltage is applied, the potential across the

semiconductor and the depletion layer width will decrease. The total potential across the semiconductor equals the built-in potential minus the applied voltage (Figure 2).

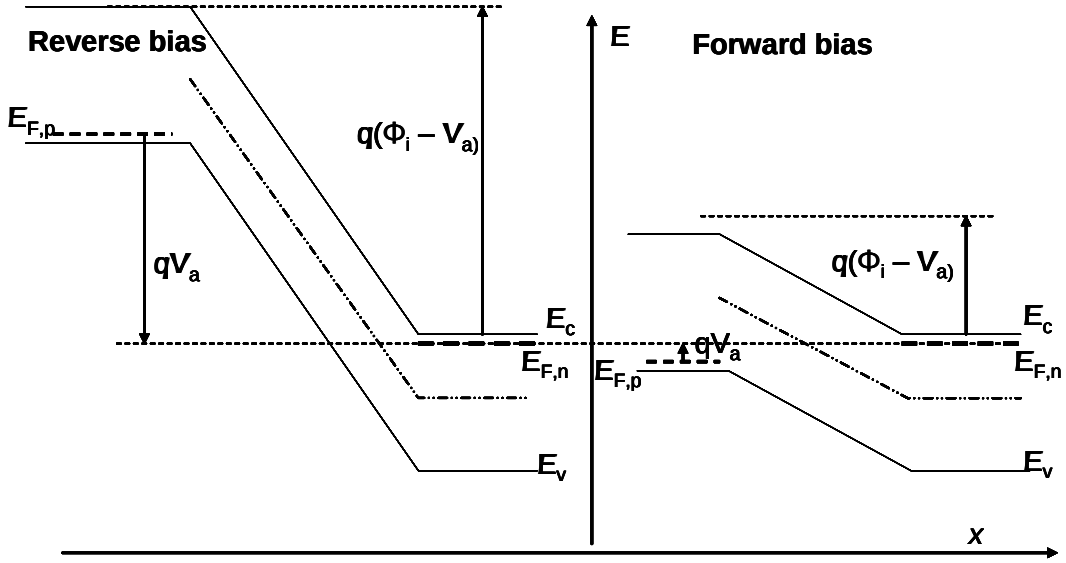

Figure 2: Schematic energy diagram of the change in energy levels when a cell is subjected to reverse and forward bias

E_c = energy at the conduction band
E_F = Fermi energy level
E_v = Energy at the valence band
N_a = Acceptor density in the *p*-type region per cm^3
N_d = Amount of donors in the *n*-type region per cm^3
n^2_i = amount of positive (or negative) charge carriers per cm^3
$V_f = k_bT/q$ (volts)
k_b = Bolzmann's constant 1.38×10^{-23} JK^{-1}
k_bT = kinetic energy in eV
q = charge of an electron 1.602×10^{-19} C

According to Kern *et al,* [1] reverse biasing a DSC is not critical for stability thus integrated modules are possible without protection diodes on each cell.

A test example of a dye solar cell was accidentally subjected to a reverse bias potential of 6 volt for a few seconds. The efficiency was immediately measured and found that the cell was dead. The following day the cell was tested again and unexpectedly it was found that a certain degree of recovery or regeneration had taken place.

In real life situations, one or more cells in a module can be partially shaded, which results in electrical mismatching in the cell. The cell is then subjected to reverse bias. The electrons then flow into the cell instead of out. This could irreversibly damage the cells if the voltage is large enough. To prevent damage to cells due to reverse bias, diodes are incorporated in the circuit to prevent any possibility of reverse bias. This research looks at the effects that reverse bias has on DSCs and the physical and chemical changes that occurred as a result of reverse bias.

Wheatley *et al.* [2] reported a similar incident but it was not pursued in so much detail. They used Raman, UV-Vis and cyclic voltammetry to determine changes that possibly took place in the cells. They concluded (cyclic voltammetry) that some irreversible oxidation process occurred inside the cell.

Dye solar cells were subjected to different reverse bias potentials (1, 2, 2.5 and 4.5 V). This paper reports on the results that were obtained for a cell that was subjected to a reverse bias potential of 2 V for 500 minutes.

Spectroscopic techniques (UV-Vis, Raman, FT-IR and SEM) were complimented by electroanalytical methods (impedance and IV-curves), and used to determine the physical and chemical changes that caused the decrease in cell efficiency.

2 EXPERIMENTAL

Various cells (at least five of each) were assembled to assure repeatable results of the tests. The cell dimensions were 8 mm $\times$ 60 mm (4.8 cm^2). The dye (figure 3) that was used in all cases was the N719 {di-tetrabutylammonium cis-bis(isothiocyanato)bis(2,2'-bipyridyl-4,4'-dicarboxylate) ruthenium(II)} as supplied by Dyesol. The ITO conductive glass was purchased from Solaronix (8Ω/square).

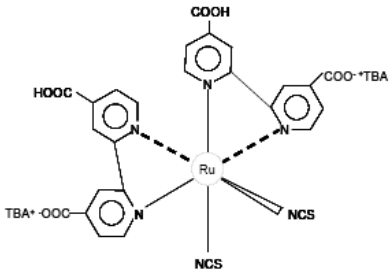

Figure 3: Structure of the N719 dye

A Perkin Elmer, Lambda 750S UV/Vis spectrometer was used to obtain the UV/Vis reflectance and absorbance spectrographs as part of the characterisation of the cells. The shift and intensity of the absorption band at 540 nm due to reverse bias was investigated, over a scan range of 400 to 700 nm at a scan rate of 266.7 nm/min and a resolution of 1 nm.

The FT-IR spectral data were collected on a Perkin Elmer Spectrum 100 FT-IR spectrometer interfaced with a Spectrum Spotlight 400 FT-IR imaging system. The changes in the NCS vibration band at 2100 cm^{-1} and C=O vibration bands at 1715 and 1354 cm^{-1} were monitored over 64 scans per sample at a resolution of 4.00 cm^{-1} in ATR (attenuated total reflectance) mode.

The Raman signal is characteristic of a particular functional group. This function would enable us to study the degradation of the dye in the cell during reverse bias [3]. Raman spectra were obtained with Jobin Yvon Lab Ram HR800 spectroscopy at room temperature, and samples were excited using the 514.5 nm line. The spot size was 150 µm and the laser power was 2 mW. The acquisition time per sample was 60 s. The microscope magnification was 10$\times$ and the system was interfaced with an Olympus BX 41 camera. The three characteristic vibration bands at 1472, 1540 and 1610 cm^{-1} were used to indicate changes in the Ru – bipyridyl bonds.

Particle and surface morphologies were studied by scanning electron microscopy using a JEOL JSM 7500F Field Emission Scanning Electron Microscope. The nano TiO_2 that was synthesised in our laboratories was compared with the P25 that was obtained from Degussa South Africa. The surfaces of the cells were compared before and after the reverse bias experiments.

The current-voltage (I-V) characteristics of the solar cells were monitored and recorded with the use of a mobile testing station for photovoltaics (MTSP purchased from Dyesol, Australia) and the solar simulator was obtained from Sciencetech (USA). The cells were scanned from -0.1 V to 0.8 V which was plotted against the current. All measurements were done under irradiation of 1 sun (1 kWm^{-2}).

The electrochemical measurements were carried out in the dark using a PGSTAT 12/30/230 potentiostat. A two electrode configuration was used where the sensitised TiO_2 was connected as the working electrode while the counter electrode (Pt), doubled as the reference electrode. The scan rate was 50 mV/s. The bias potentials ranged from -0.7 V to +0.7 V.

3 RESULTS AND DISCUSSION

3.1 Reverse bias and recovery

The results of four identical cells that were subjected to different reverse bias voltages and the efficiencies were plotted against time are shown in figure 4. Reverse bias voltages of 1 V (blue); 2 V (Magenta); 2.5 V (black); and 4.5 V (brown) were used in the experiments.

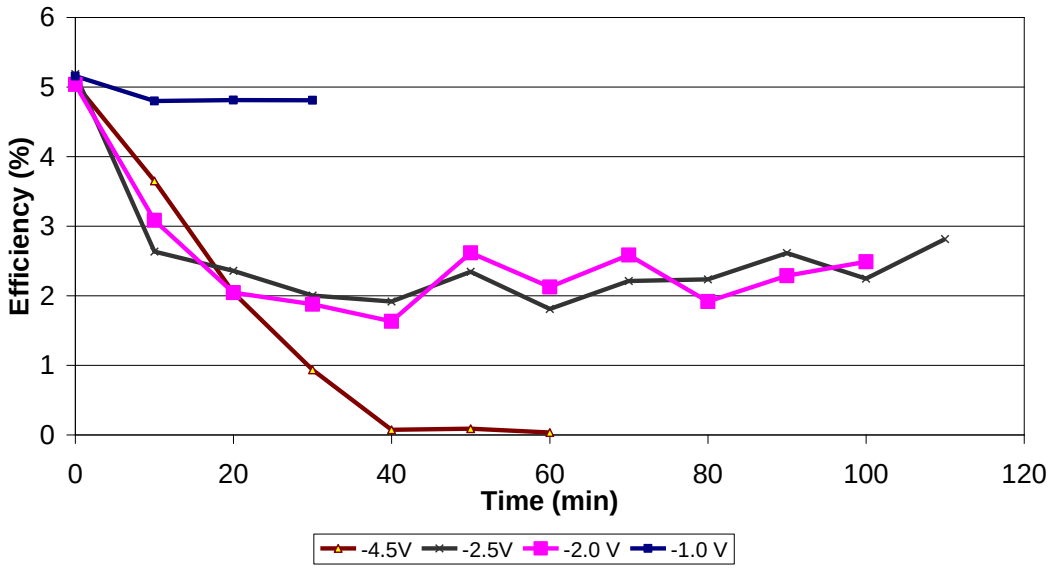

Figure 4: Efficiencies plotted during subjection to different reverse bias voltages. Measurements were taken at 10-minute intervals. Note the similar results for 2 and 2.5 V.

Under a reverse bias of 1 V, there is little reduction in the efficiency of the cell. The drop in efficiency from 5.1 to 4.8% is 0.3% (5.9% overall).
Figure 4 shows that there was no meaningful difference when the cells were subjected to reverse bias voltages of 2 and 2.5 V. The results for the 2.5 V reverse bias experiments will therefore not be discussed further in this document.
When the cell was subjected to a reverse bias potential of 4.5 V, the efficiency dropped to 0% in 50 minutes.

A cell was subjected to a reverse bias potential of 2 V and the efficiency was measured at different time intervals to determine the rate of degradation. The regeneration was measured against time after the reverse bias voltage was removed. The efficiencies were plotted against time (see Figure 5).

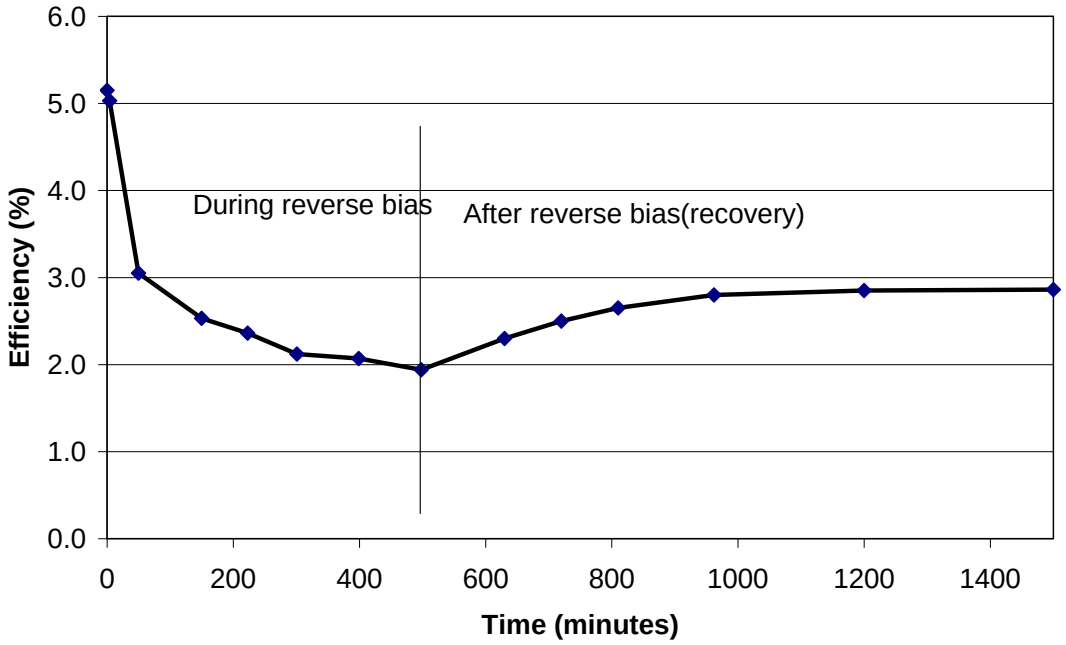

Figure 5: A plot of efficiency vs. time for a cell that was subjected to a reverse bias of 2 V for 500 minutes after which the cell's recovery was monitored.

The efficiency of the cell decreased from 5.1% to 2% after 500 minutes. When the reverse bias potential was removed, the cell recovered partially to give a final efficiency of 2.9%.

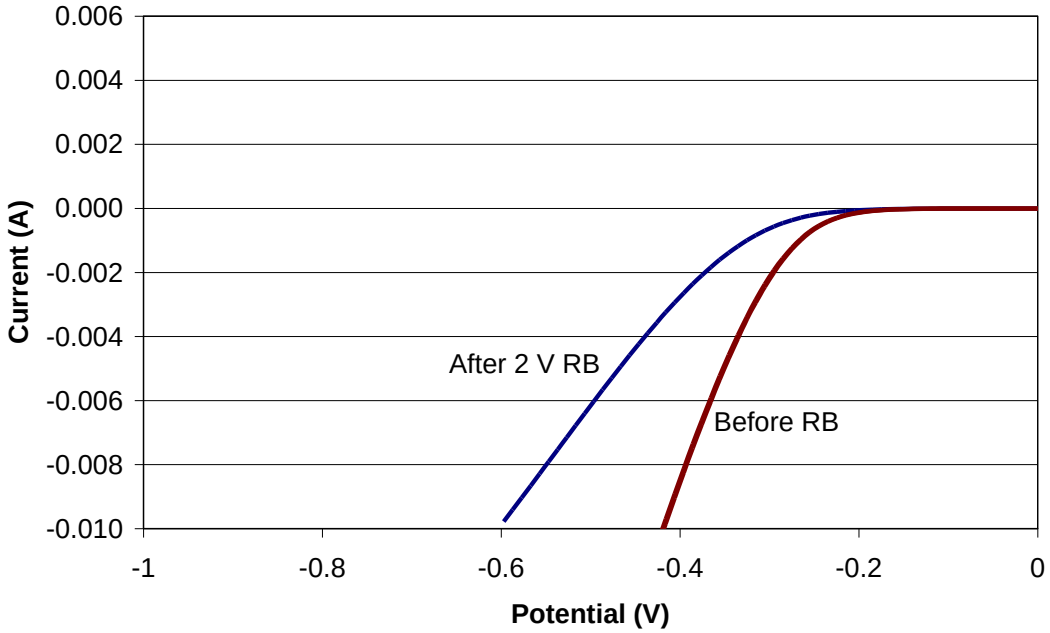

Figure 6: The IV curves for the cells (negative voltages only).
The blue line represents the cell that was not subjected to any reverse bias. The red line is the cell that was subjected to 2 V reverse bias.

The data from the graph (figure 6) was used to determine the different values for the exchange current density. This was compared with the curve of the cell before reverse bias. The Butler-Vollmer model is only valid in reverse bias (V<0)[4].

$$J(V) = J \circ \underbrace{\left(\exp\left(\beta \frac{qV}{kT} \right) \right)}_{\sim 0 \; for V<0} \tag{1}$$

Applying the experimental data to the simplified Butler-Volmer equation, the following values were calculated for J_0 (exchange current density). The symmetry factor (β) was taken as 0.5. J_0 is indicative of the rate of oxidation or reduction at an equilibrium electrode. J_0 for the cells were determined as:

Before reverse bias: 7.2×10^{-11} A/cm^2; After 2 V reverse bias: 8.8×10^{-13} A/cm^2

The reaction rate after the cell was subjected to a reverse bias potential of 2 V was about three times less than the cell before reverse bias.

3.2 Efficiency measurements

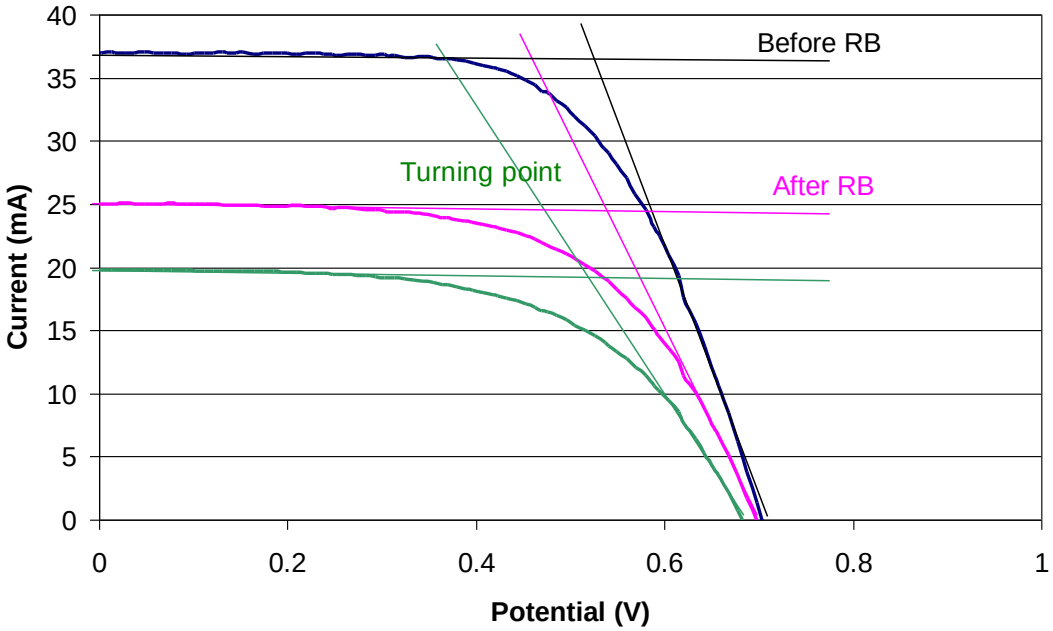

Figure 7: IV curves for the cell during and after being subjected to a reverse bias of 2 V. The blue trace is the efficiency before reverse bias while the recovered is indicated by the magenta trace. The green trace represents the turning point before recovery. The slopes of the I_{sc} and V_{oc} are also indicated on the graph.

The IV curves shown in figure 7 were obtained during the time that the cell was subjected to reverse bias. The blue traces are during reverse bias while the recovery is indicated by the magenta traces. Although there was a significant change in the I_{sc}, the V_{oc} showed only a small variation.
The inverse of the slopes of the curve that indicates R_{sh} and R_s are shown in table 1.

Table1: Shunt and series resistances as calculated from the IV-curves

	R_{sh} (Ω)	R_s (Ω)
Before reverse bias	3324	4.3
Minimum efficiency (turning point)	2517	7.6
After recovery	3247	5.8

These values show the same trends that were found when the modelling was done for the equivalent circuits (see table 2).

3.3 Impedance measurements

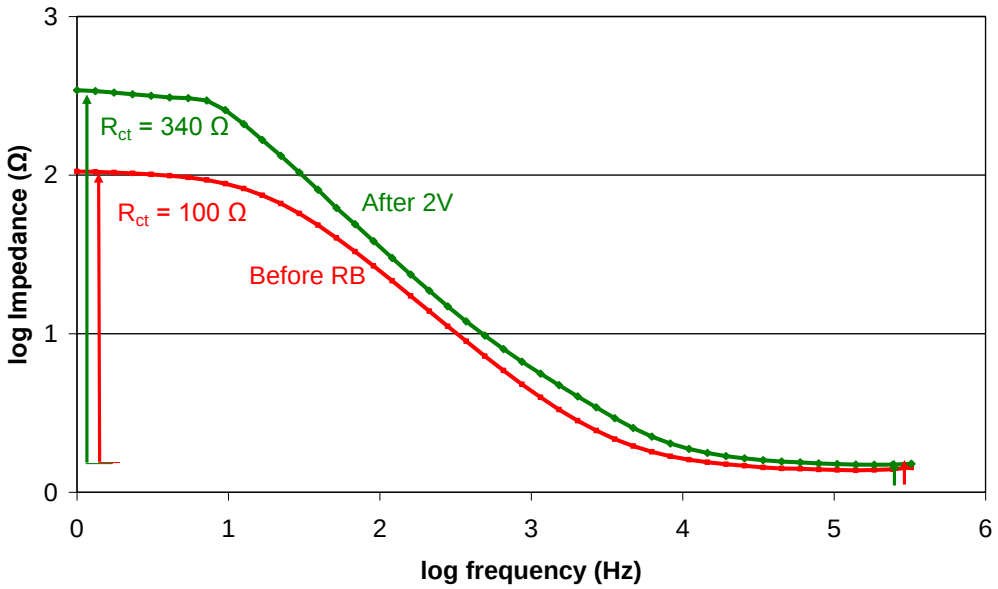

Figure 8: Bode plots of the cell before reverse bias (red) and after 2 V reverse bias (green).

Note there is no significant change in the series resistance (R_s), indicated on the right hand side of the graph in figure 8. Both start at 1.4 Ω. After the cell was subjected to 2 V reverse bias, the charge transfer resistance (R_{ct}) increased to 340 Ω.

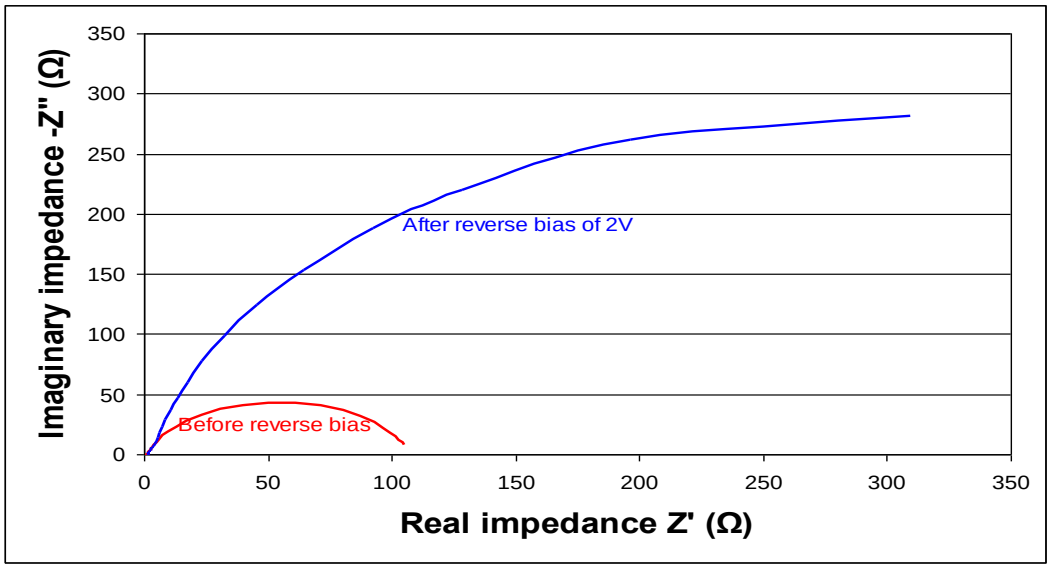

Figure 9: Nyquist plots of the cell before reverse bias (red), after 2 V reverse bias (blue).

The increase in impedance shown in figure 8 also correlates with the trends of increase in impedance that is depicted in the Bode plots (figure 8). Figure 10 shows the Nyquist plots as well as the equivalent circuits of the cells before and after reverse bias.

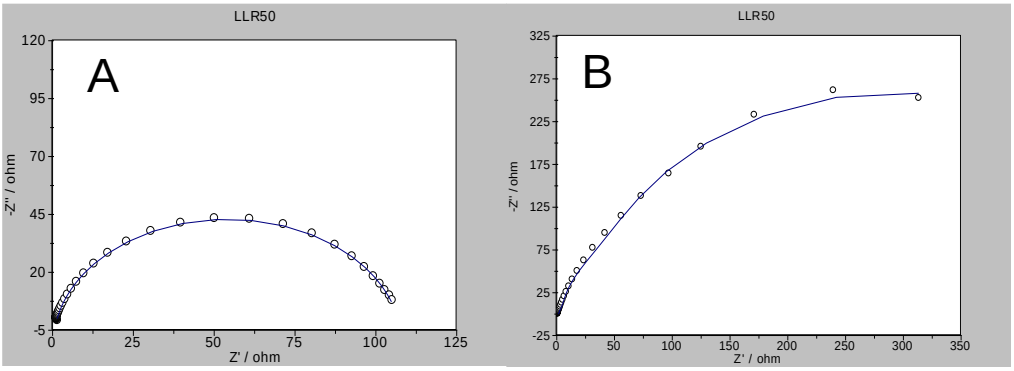

Figure 10: Nyquist plots of the cells cell before (A) and after (B) reverse bias. The blue lines show the theoretical fit of the equivalent circuit in each case.

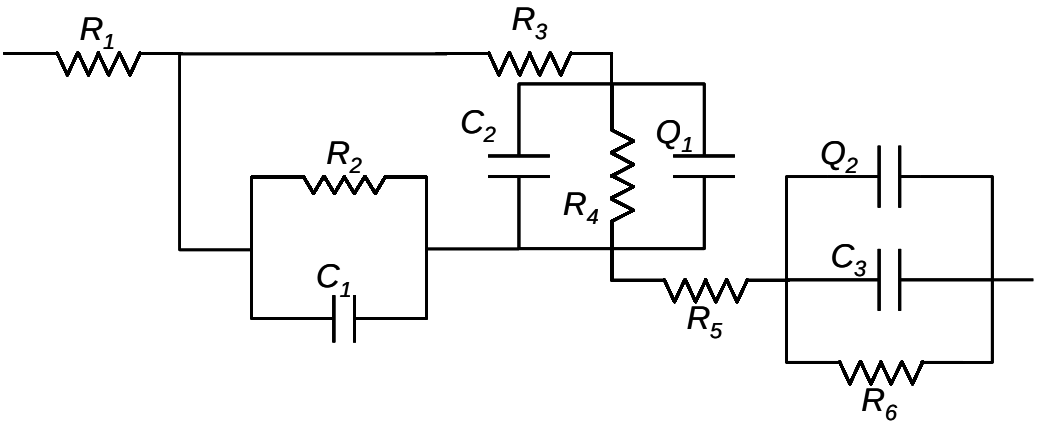

Figure 11: Equivalent circuit of a cell before and after reverse bias

The equivalent circuits for both cases are essentially the same as shown in figure 11. The circuits give a good fit as shown in the Nyquist plots (figure 10). The calculated values of the components (before and after reverse bias) that are derived from these models are compared in table 2.

The part of the circuit that is shown as R_2, represents the charge transfer resistance for electron recombination at the TiO_2/ITO interface in the cell while C_1 represents the capacitance at the triple contact ITO/TiO_2/electrolyte.

$C_2/R_4/Q_1$ represents the charge-transfer resistance (R_4) due to the recombination of electrons at the TiO_2/electrolyte interface, the chemical capacitance (C_2) and constant phase element (Q_1) due to a change in electron density. (The first indication that a constant phase element exists is that the centre of the semi circle in the Nyquist plot has shifted to below the x-axis.) This is evident in both plots in figure 9.

R_3 and R_5 represent the electron transport resistance in the TiO_2 layer. $C_3/Q_2/R_6$ represents the capacitance and charge transfer resistance as well as the constant phase element at the electrolyte/platinum interface in the cell.

Table 2: Numerical values (based on the model of the Nyquist plot) of the different components of the cells before and after reverse bias.

	Before reverse bias	After reverse bias of 2 V
R_1	4.73 Ω	4.73 Ω
C_1	1.00 pF	1.00 pF
R_2	12.8 mΩ	15.4 mΩ
R_3	4.73 Ω	4.73 Ω
C_2	22.8 µF	1.00 pF
R_4	46.8 Ω	146 Ω
Q_1	4.40×10^{-4}	7.98×10^{-4}
n_1	0.833	0.827
R_5	4.73 Ω	4.73 Ω
C_3	10.6 µF	1.00 pF
Q_2	4.46×10^{-4}	7.97×10^{-4}
n_2	0.834	0.829
R_6	61.3 Ω	208 Ω

R_1, R_3 and R_5 are the series resistance components of the cell and showed no change before or after reverse bias of 2 V. The major differences appear to be with the charge transfer resistance (R_2, R_4 and R_6) that indicates that physical changes took place inside the cell as well as at the counter electrode.

The charge transfer resistance at the electrolyte/platinum interface increased from 61 Ω to 208 Ω. Work that was done by Milkevitch *et al.* [5] indicated that the platinum catalyst can be irreversibly oxidised at voltages of 1.72 V and 1.61 V. The value of the constant phase elements Q_1 and Q_2 doubled while the value of n only increased slightly from 0.827 to 0.833 which relates to 0.5° change in the phase. The capacitance inside the cell (C_2 and C_3) has decreased significantly while the capacitance at the working electrode stayed constant.

3.4 UV-vis measurements

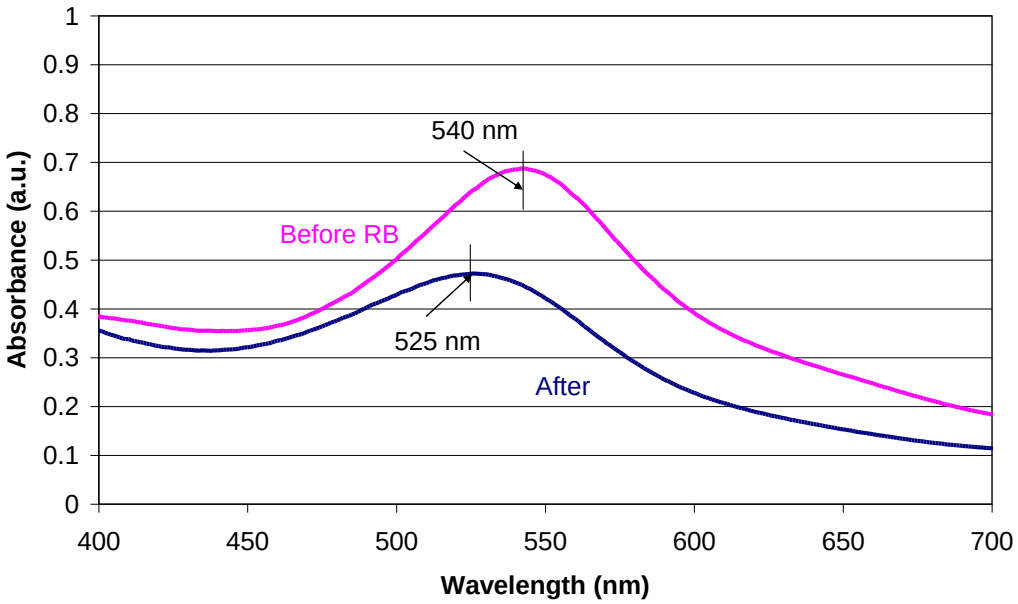

Figure 12: UV-Vis results of a cell before and after reverse bias. Note the peak shift from 540 to 525 nm.

When a reverse bias potential of 2 V was applied to the cell the absorption band at 540 nm shifted to 525 nm with a reduction in absorptivity (figure 12). This absorption band is due to the metal-to-ligand charge transfer (MLCT) from the Ru metal centre to π* orbitals on the pyridyl ligand. The molecule is stabilised by the delocalising effect of the electron donating N-C-S groups. The band shifted to higher energy (blue shift) which resulted in lower cell efficiency.
The absorbance decreased from 0.68 to 0.47 (30%). The decrease in cell efficiency was 42% (from 5.1% to 2.9%) which suggests that this is not the only parameter that changed during the reverse bias.
It was previously determined by Murakoshi *et al*., [6] that the absorption shifts to lower energies when the complexes are attached to the semiconductor surface. The band shifts were ascribed to the interaction between the dye molecule and the TiO_2 surface through the carboxylic groups. This leads to the possible conclusion that some of the dye was desorbed from the TiO_2 during the reverse bias experiments.
The blue shift could therefore be a combination of the breaking of bonds between the dye and the TiO_2 and the depletion of the N-C-S groups. It was confirmed by FT-IR and Raman that there is no evidence of bond breaking between the TiO_2 and the dye therefore the shift has to be due to the depletion of the N-C-S groups.

3.5 Raman measurements

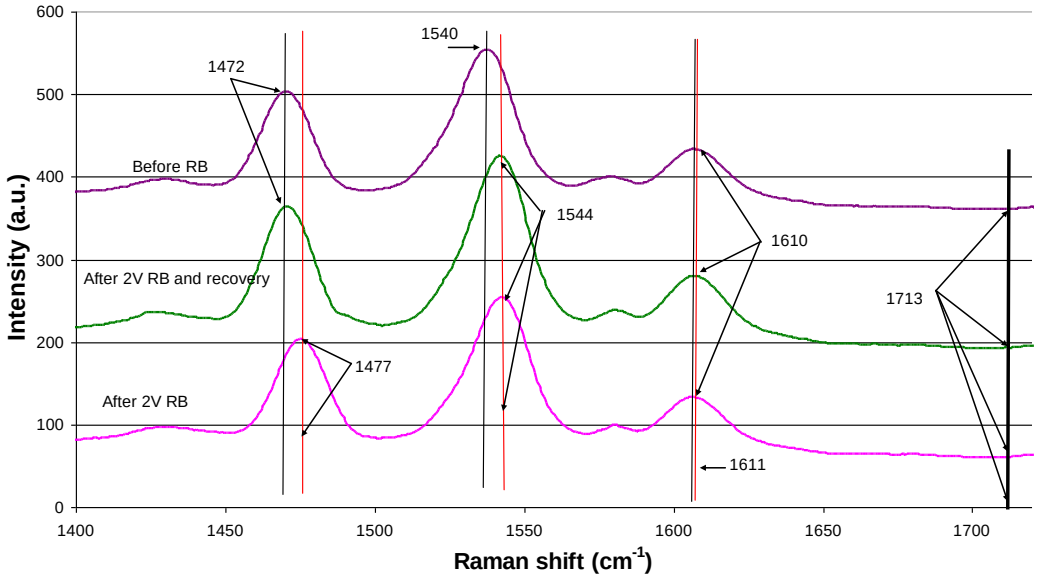

Figure 13: Raman spectra of a cell that was subjected to a reverse bias voltage of 2 V. Note the peak shifts in the original spectrum before reverse bias, after 2 V reverse bias (before and after recovery). Note the absence of peaks at 1713 cm^{-1}.

The absence of the characteristic C=O stretch band at 1713 cm^{-1} is an indication that there are no free C=O groups in the cell. This proves that the dye is not desorbed from the titanium dioxide surface. FT-IR spectroscopy measurements also indicated that no desorption of the dye from the TiO_2 film occurred. During the application of reverse bias potentials, the peaks at 1540 and 1472 cm^{-1} shifted by 5 and 4 cm^{-1} respectively to higher energy while the energy of the band at 1610 cm^{-1} was essentially unchanged (figure 13). After reverse bias and recovery (2 V), the 1472 cm^{-1} band returned to the original value but the peak initially at 1540 cm^{-1} remained displaced by 4 cm^{-1} to higher energy. The irreversible change to the band at 1540 cm^{-1} suggests that the adsorbed dye has undergone a change directly associated with the bipyridyl ligand.

3.6 FT-IR measurements

The FT-IR measurements showed n No evidence could be found of any desorption of the dye carbonyl group from the TiO_2. If there were any isolated (not bound to TiO_2) carbonyl groups, vibrational bands at wavenumbers 1354 and 1715 cm^{-1} should become evident. This however is not the case. The strong bands at 1375 cm^{-1} and 1635 cm^{-1} indicate bonded carbonyl groups. Therefore with the FT-IR spectral data we can state that there is no disengagement of the dye from the TiO_2 (figure 14). This is also confirmed by results that were obtained by Kuang *et al*.[7].

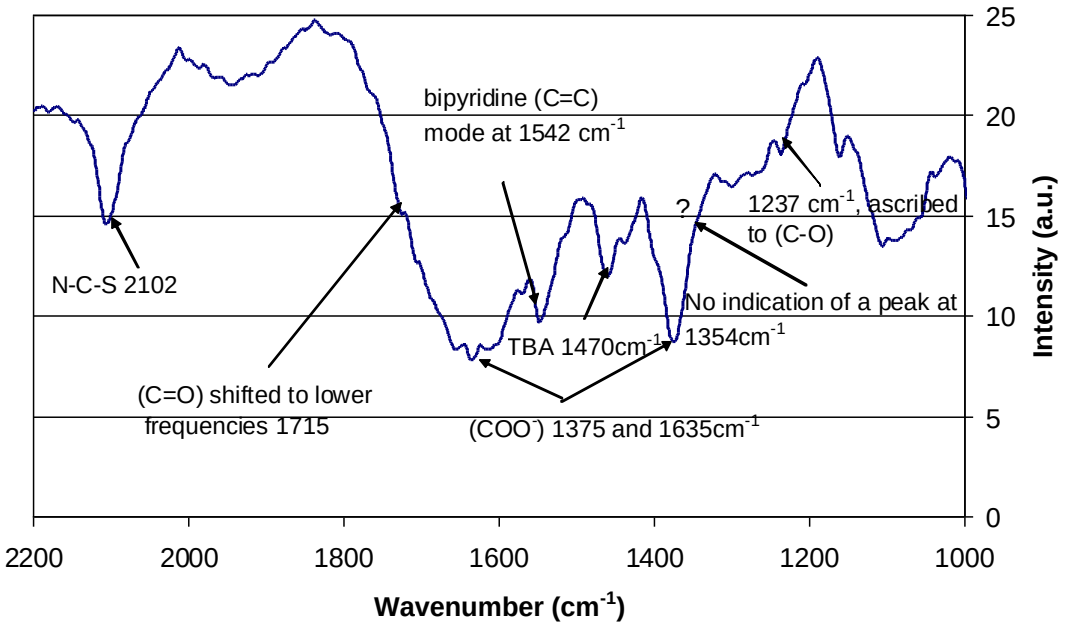

Figure 14: FT-IR spectrum of the dye after being subjected to a reverse bias voltage of 2 V.

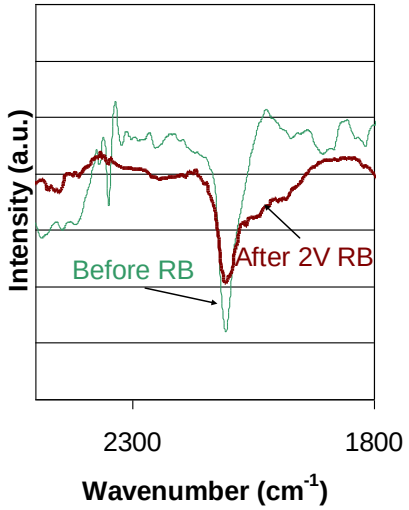

Figure 15: The FT-IR spectrum of the cells before and after a reverse bias (RB) voltage of 2V. Note the decrease of the intensity of the CN peak at 2100 cm^{-1}.

The spectra in figure 15 show the effect of the 2 V reverse bias on the N-C-S group in the dye. The N-C-S stretching band is slowly depleted. It seems as if the thiocyanate ion ligand is sensitive to the oxidizing effect of the reverse bias on the N-C-S groups. It was suggested by Greijer *et al*., [8] that a compound analogue to the I_3^- forms:

$$I_2 + SCN^- \rightarrow I_2SCN^-$$

This strongly correlates with the decrease in intensity and blue shift in the UV–Vis absorption bands and is attributed to the destabilising effect of the depleting N-C-S group.

3.7 SEM measurements

SEM photos (magnification for both were 30.00 K X) were obtained before and after the reverse bias potential of 2 V as shown in figure 16. No obvious changes or differences could be detected. This confirms that the morphology did not change due to the reverse bias. The surface porosity of the two films does not show any visible or obvious change.

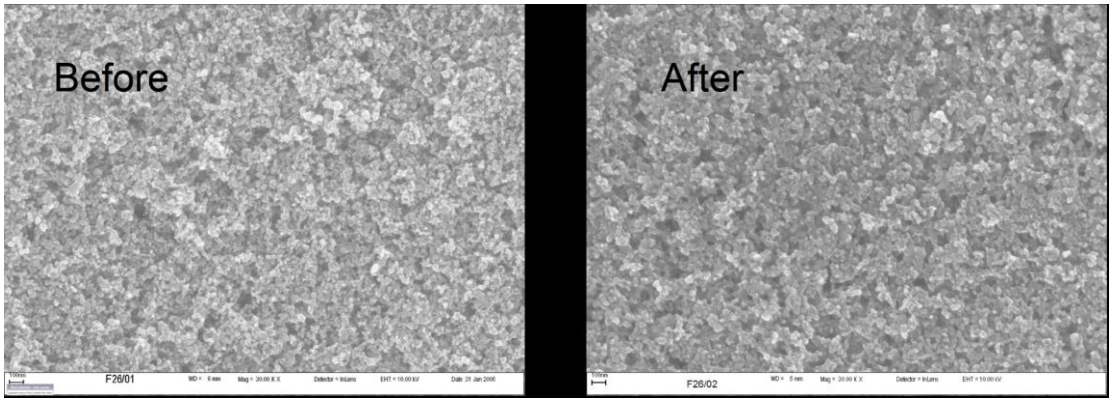

Figure 16: SEM micrograph of the TiO_2/dye of a cell before and after reverse bias.

4 CONCLUSIONS

We have shown that a reverse bias potential of 2 V resulted in a 42% loss in cell efficiency.
Raman spectroscopy showed the partial recovery of the cell at 2 V reverse bias. The appearance of a vibration band at 1713 cm^{-1} would be evidence of the breaking of the chemisorbed bonds between the dye and the TiO_2 film (dislocation of the dye and the TiO_2). This was not the case and it was also backed up by FT-IR measurements showed no peaks at 1715 cm^{-1} and 1354 cm^{-1} which is characteristic of free carbonyl bonds.
FT-IR however did show the depletion of the N-C-S vibration band at 2100 cm^{-1}.
This work has shown that Raman and FT-IR spectroscopy are complementary techniques that provided structural information of the dye and dye/semiconductor system.

Potentiometric measurements show a significant increase in the charge transfer resistance at the counter electrode which indicates a decrease in the catalytic activity of the Pt. This backs the theory of Milkevitch *et al.*[9] that there is partial oxidation of the Pt that acts as a catalyst for the regeneration of the Iodide. It was shown by FT-IR that the change was in the dye and not the TiO_2/dye bond.
The values of R_s and R_{sh} that were obtained from the IV curves of the cell under reverse bias showed the same trends that were obtained from the Nyquist plots, Bode plots and equivalent circuits.

It can therefore be stated with confidence that the changes in the cell after being subjected to a reverse bias potential of 2 V for 500 minutes are attributed to changes on the N-C-S groups on the Ru dye as well as the Pt on the counter electrode.
The morphology of the TiO_2 film on the glass substrate does not change when a cell is subjected to a reverse bias potential of 2 V.

5 ACKNOWLEDGEMENTS

Dr Mkhulu Mathe (Council for Scientific and Industrial Research)
Dr Kenneth Ozoemena (Council for Scientific and Industrial Research /University of Pretoria)
Ms Nonhlanhla Mphahlele (Council for Scientific and Industrial Research)

Ms Nomthandazo Mutangwa (Council for Scientific and Industrial Research)
Dr Paul Sommeling (Energy Research Centre of the Netherlands)

6 REFERENCES

[1] Kern R, Sastrawan R, Ferber J, Stangl R, Luther J (2002) Modelling and interpretation of electrical impedance spectra of dye solar cells operated under open-circuit conditions. Electrochimica Acta 47 4213-4225.

[2]. Wheatley MG, McDonagh AM, Brungsa MP, Chaplina RP and Sizgekc E (2003) A study of reverse bias in a dye sensitised photoelectrochemical device. Solar Energy Materials & Solar Cells 76 175–181

[3]. Gao K and Wang D (2007) Raman study of photo-induced degradation of the Ru(II) complex adsorbed on nanocrystalline TiO_2 films. Phys. Status Solidi RRL 1(2) R83-R58

[4]. Hinsch A, Belledin U, Brandt H, Einsele F, Hemming S, Koch D, Rau U, Sastrawan R and Schauer T (2006) Glass Frit Sealed Dye Solar Modules With Adaptable Screen Printed Design. Paper presented at the 4th World Conference on Photovoltaic Energy Conversion: Hawaii

[5]. Milkevitch M, Brauns E and Brewer KJ (1996) Spectroscopic and Electrochemical Properties of a Series of Mixed-metal d^6,d^8 Bimetallic Complexes of the Form $[(Bpy)_2m(BL)PtCl_2]^{2+}$ (Bpy = 2,2'-Bipyridine; BL = dpq (2,3-Bis(2- Pyridyl)Quinoxaline) Or dpb (2,3-Bis(2-Pyridyl)- Benzoquinoxaline); M = Os^{ii} Or Ru^{ii}). Inorg Chem 35 (6) 1737-1739

[6]. Murakoshi K, Kano G, Wada Y, Yanagida S, Miyazaki H, Matsumoto M and Murasawa S (1995) Importance of binding states between photosensitizing molecules and the TiO_2 surface for efficiency in a dye-sensitized solar cell. J Electroanal Chem 396 27-34

[7]. Kuang D, Ito S, Wenger B, Klein C, Moser J, Humphry-Baker R, Zakeeruddin SM, Grätzel M (2006) High Molar Extinction Coefficient Heteroleptic Ruthenium Complexes for Thin Film Dye-Sensitized Solar Cells. J Am Chem Soc 128 (12) 4146-4154

[8]. Greijer H, Lindgren J and Hagfeldt A (2001) Resonance Raman Scattering of a Dye-Sensitized Solar Cell: Mechanism of Thiocyanato Ligand Exchange. J Phys Chem B 105 6314-6320

[9]. Milkevitch M, Brauns E and Brewer K.J (1996) Spectroscopic and Electrochemical Properties of a Series of Mixed-metal d^6,d^8 Bimetallic Complexes of the Form $[(Bpy)_2m(BL)PtCl_2]^{2+}$ (Bpy = 2,2'-Bipyridine; BL = dpq (2,3-Bis(2- Pyridyl)Quinoxaline) Or dpb (2,3-Bis(2-Pyridyl)- Benzoquinoxaline); M = Os^{ii} Or Ru^{ii}). Inorganic Chemistry 35 (6) 1737-1739